" Campo Laborde: A Late Pleisto-
cene giant ground sloth kill and
butchering site in the Pampas"

G.G. Politis *et al.*

eaau4546

ANTHROPOLOGY

Campo Laborde: A Late Pleistocene giant ground sloth kill and butchering site in the Pampas

Gustavo G. Politis[1]*, Pablo G. Messineo[2], Thomas W. Stafford Jr[3], Emily L. Lindsey[4]

The extinction of Pleistocene megafauna and the role played by humans have been subjects of constant debate in American archeology. Previous evidence from the Pampas region of Argentina suggested that this environment might have provided a refugium for the Holocene survival of several megamammals. However, recent excavations and more advanced accelerator mass spectrometry radiocarbon dating at Campo Laborde site in the Argentinian Pampas challenge the Holocene survival of Pleistocene megamammals and provide original and high-quality information documenting direct human impact on the Pleistocene fauna. The new data offer definitive evidence for hunting and butchering of *Megatherium americanum* (giant ground sloth) at 12,600 cal years BP and dispute previous interpretations that Pleistocene megamammals survived into the Holocene in the Pampas.

INTRODUCTION

The late Quaternary megafaunal extinctions at the end of the Pleistocene, resulting in the loss of between 35 and 90% of large-bodied animal species on ice-free continents (excluding Africa), represented the most profound faunal transition that Earth's ecosystems experienced during the Cenozoic, but the cause or causes of this event remain hotly debated (*1*–*4*). In the New World, the causes and dynamics of the extinctions have proved especially challenging to elucidate because they coincided closely both with end-Pleistocene climate changes and with the invasion of a new predator—*Homo sapiens* (*2, 3, 5, 6*). Understanding this extinction in South America, both in archeology and paleontology, has suffered primarily from a lack of chronological control for the disappearance of megafauna taxa, as well as data on the extent of their temporal overlap and interactions with humans (*3, 4, 7*–*9*).

South America is particularly important for investigations of late Quaternary extinctions because the continent lost more megafauna taxa than any other continent during this event (*2, 3, 9, 10*). The answer to the questions of the underlying causes may reveal fundamental principles of ecology—are extinctions synchronous across species, are they abrupt or gradual, why do some taxa survive in refugia while the majority are lost, and can a single new species disrupt ecosystems in equilibrium for hundreds of millennia?

Previous studies of the late Quaternary extinctions in South America have found evidence for both human-driven (*11*) and climate-driven (*12*) megafauna loss, as well as synergistic impacts of these two factors (*3, 13*). However, direct evidence of human predation on extinct megafauna in South America is rare (*8*), despite thousands of years of apparent overlap in some regions (*9*) and evidence that some taxa could even have survived into the Holocene (*10, 14, 15*).

We use the Argentinian archeological site, Campo Laborde, to demonstrate that humans hunted and butchered a giant ground sloth, that advanced radiocarbon dating techniques do not support Holocene survival of megafauna in the area, and that these new

dates cast doubts on other published Holocene ages for Pleistocene fauna in the Pampas.

The essential data for assessing the interactions of fauna, climate, and humans are accurate chronologies for extinctions, climate changes, and the timing and rates of human dispersals. These data must derive from well-dated archeological sites having indisputable association with remains of extinct taxa (*16*–*18*). While most New World archeological sites with unquestionable extinct megafauna have Late Pleistocene dates [~14,500 to 13,000 cal years before the present (BP)], some sites in the South America Pampas (Fig. 1A) have been dated to the Early and Middle Holocene (*10, 19*–*23*), thereby causing archeologists and paleontologists to question the impact of humans on Late Pleistocene extinctions (*3, 7, 15*). Besides Campo Laborde, archeological sites that supported Holocene survivals of megafauna include La Moderna (*19*), Arroyo Seco 2 (*18, 24*), and Paso Otero 4 (*22*), as well as paleontological localities that yielded Early Holocene dates on extinct megamamals such as Arroyo Tapalqué (*10*) and Río Cuarto (*25*).

Of these sites, La Moderna has provided the greatest number of Early and Middle Holocene dates. It is an open-air site located on the banks of the Azul Creek (Fig. 1A), where a close stratigraphic association between lithic artifacts (expedient tools of crystalline quartz and some curated tools of orthoquartzite and chert) and extinct faunal remains [*Doedicurus clavicaudatus* (Glyptodontidae)] was confirmed (*19*). La Moderna is interpreted as a procurement site, where, during a single event, a *D. clavicaudatus* was butchered at the edge of an ancient swamp (*19*). The chronology of this event has always been problematic and controversial. For these reasons, multiple samples have been run on *D. clavicaudatus* bone collagen and organic sediment samples. The first dating result was a standard age processed by Beta Analytic and yielded an age considered to be too young: 6550 ± 160 ^{14}C years BP (Beta-7824). A second bone sample yielded an accelerator mass spectrometry (AMS) age of 12,350 ± 370 ^{14}C years BP (TO-1507) through the IsoTrace Lab. Two additional dates from the same bone from the same laboratory with a more appropriate pretreatment yielded ages of 7010 ± 100 ^{14}C years BP (TO-1507-1) and 7510 ± 370 ^{14}C years BP (TO-1507-1). Last, radiocarbon dating a third bone fragment gave a result close to these ages [7460 ± 80 ^{14}C years BP (TO-2610)]. Two organic samples were taken from lithostratigraphic unit (a′), which contained the archeological deposit produced ages of 8356 ± 65 ^{14}C years BP (DRI-3012) and 7448 ± 109 ^{14}C years BP [DRI-3012 (*19, 26*)]. As a consequence,

[1]INCUAPA-CONICET, Facultad de Ciencias Sociales (UNICEN) and Facultad de Ciencias Naturales y Museo (UNLP), Olavarría, Buenos Aires B7400JWI, Argentina. [2]INCUAPA-CONICET, Facultad de Ciencias Sociales (UNICEN), Olavarría, Buenos Aires B7400JWI, Argentina. [3]Stafford Research LLC., Lafayette, CO 80026-1845, USA. [4]La Brea Tar Pits and Museum, Los Angeles, CA 90036, USA.
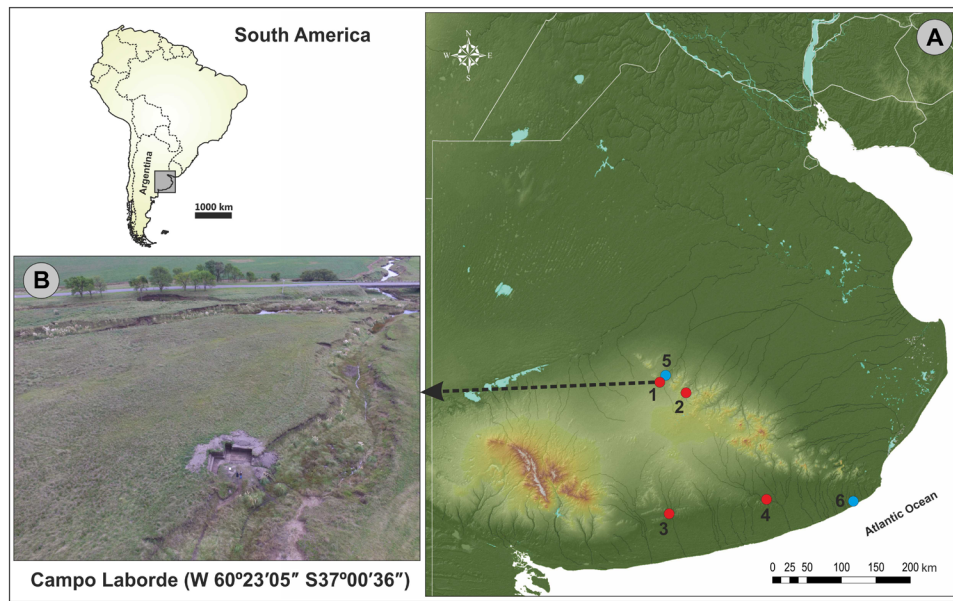*Corresponding author. Email: gpolitis@fcnym.unlp.edu.ar

Fig. 1. Location of Campo Laborde site in South America. (**A**) Map of the Pampas grassland of Argentina (province of Buenos Aires), showing main sites mentioned in the text. References: 1, Campo Laborde site; 2, La Moderna site; 3, Arroyo Seco 2 site; 4, Paso Otero 4 and 5 sites; 5, Arroyo Tapalqué; 6, Centinela del Mar; red circles, archeological sites; blue circles, paleontological sites. (**B**) Aerial view of excavation area, picture courtesy of C. F. Dubois. [Photo credit: Dr. Cristian Favier Dubois. INCUAPA-CONICET, Facultad de Ciencias Sociales (UNICEN)].

this series of dates suggested that the age of La Moderna was between 7000 and 7500 ^{14}C years BP. The 6550 ± 160 ^{14}C years BP date was considered too young, while the 12,350 ± 370 ^{14}C years BP age was discarded as too old; both dates were considered as outliers (*26*).

The other site with Holocene dates on extinct fauna is Arroyo Seco 2. The site presents abundant evidence related to the study of the Pleistocene megafauna (*7, 18, 24*). This multicomponent, open-air locality lies between a low ridge of loess and a small stream, Arroyo Seco Creek (Fig. 1A). The Arroyo Seco 2 site has an early component containing a lithic assemblage composed of unifacial, marginally retouched tools associated with bone remains of nine extinct taxa: *Equus neogeus*, *Hippidion* sp., *Toxodon platensis*, *Megatherium americanum*, *Eutatus seguini*, *Glossotherium robustum*, *Macrauchenia* sp., *Glyptodon* sp., and Camelidae cf. *Hemiauchenia* (*18*). Three extinct species found in the early component show evidence of human exploitation: *E. neogeus*, *Hippidion* sp., and *M. americanum*. The lower component of Arroyo Seco 2 is interpreted to be the result of several, low-resolution, human occupations at the end of the Pleistocene. In the late 1980s and early 1990s, three radiocarbon ages from bone collagen of *E. (Amerhippus) neogeus* and *M. americanum* yielded Early Holocene ages: 8890 ± 90 ^{14}C years BP (TO-1504), 8470 ± 240 ^{14}C years BP (LP-53), and 7320 ± 50 ^{14}C years BP [TO-1506 (*7*)]. However, 15 AMS ages on megafauna bones, from different taxa, from Arroyo Seco 2 run at different radiocarbon laboratories yielded ages between 12,240 ± 110 ^{14}C years BP and 10,500 ± 90 ^{14}C years BP (*18*). Among these, three new results were particularly substantial as they were obtained on the same *M. americanum* bone sample previously dated to 7320 ± 50 ^{14}C years BP. These new results negate the Holocene age of the sample and place it at the end of the Pleistocene: 12,200 ± 170 ^{14}C years BP (CAMS-58182), 12,155 ± 70 ^{14}C years BP (OxA-10387), and 11,770 ± 120 ^{14}C years BP (AA- 62514). Therefore, the 7320 ± 50 ^{14}C years BP and 8470 ± 240 ^{14}C years BP measurements should both be rejected. The age of 8890 ± 90 ^{14}C years BP from *E. neogeus* was also not replicated. Four ages, from separate

bone samples of *Equus*, gave Late Pleistocene ages [between 11,320 ± 110 ^{14}C years BP (AA-39365) and 11,000 ± 100 ^{14}C years BP (OxA-4590)]. As a consequence, the new group of radiocarbon dates from Arroyo Seco 2 does not appear to support a Holocene fauna survival at the site as previously proposed (*7*), with the exception of medium-sized *E. seguini* [dated in 7388 ± 74 ^{14}C years BP (AA-90117)] (*18*).

The third site with a purported Holocene age is Paso Otero 4 (Fig. 1A). There are no direct dates on extinct faunal bones despite several failed attempts. The only dates for Paso Otero 4 are Early Holocene ^{14}C dates on humates [between 8913 ± 49 ^{14}C years BP (AA-87938) and 7729 ± 48 ^{14}C years BP (AA-85157)] from the lower unit 2 containing *E. seguini* bones (*22*). Other [14]C Holocene dates from extinct fauna in the Pampas (Fig. 1A) include two dates on *Scelidotherium leptocephalum*, one of 7615 ± 85 ^{14}C years BP (GrA-48388) from Arroyo Tapalqué (*10*) and another of 7550 ± 60 ^{14}C years BP (LP-1407) from Río Cuarto (*25*). Last, an age of 9890 ± 50 ^{14}C years BP (GrA-49321) was reported for *Macrauchenia patachonica* from Centinela del Mar (*10*).

The Campo Laborde site can provide high-quality data for discussing the human impact on the Pleistocene fauna and the timing of the megamammal extinctions in the Pampas and in South America due to its good stratigraphic resolution and high-accuracy radiocarbon dates. The site is located in the upper basin of Tapalqué Creek, ~15 km north-northeast of Olavarría city (Pampas region of Argentina; Fig. 1, A and B). In 2000, the landowner discovered in situ a complete femur and vertebrae fragments from a giant ground sloth, *M. americanum*. The original test pits were started here, and the site was expanded with subsequent excavations during two field programs. The first was between 2001 and 2003, when an area of 29 m^2 was excavated (*20, 21*). The second field session was in 2016 and 2017, when a new area of 21 m^2 was excavated. This report presents and integrates the findings of the 2016–2017 field seasons and includes the new radiocarbon dates made with more advanced and accurate methods for radiocarbon dating bone.

RESULTS

The 2001–2003 excavations uncovered a great amount of giant ground sloth bones associated with lithics and only two glyptodont bones (Fig. 2 and fig. S1) in swamp sediments between 1.00 and 1.30 m below ground level (BGL). Approximately 70% of the lithic artifacts were found among the megamammal bone concentration, while the remaining percentage was recovered around the concentration but in sectors very close to the bones (fig. S2). We made the statistical test correlation between the frequency of spatial distribution of lithics and bones. As a result, we find a positive and significant correlation (Spearman's rho = 0.454, $P = 0.00072$) supporting an intimate spatial association between bones and cultural remains. Lithic material included a lanceolate bifacial projectile point stem, a broken side scraper, one orthoquartzite flake, and 128 orthoquartzite, silicified dolomite, and chert microflakes ranging from 2 to 9 mm long (27). The artifact interpreted as the base of a broken lanceolate bifacial projectile point (FCS.CLA.33) has a convex bottom, a transverse distal fracture (Fig. 3A), and edges with no intentional abrasion (28). Use-wear analysis indicates that both edges have postdepositional alterations (e.g., soil sheen), and for this reason, they do not show diagnostic characters associated with the tool's use. One face of this point has laminar pressure-flaked scars along the base, and the opposite face has a single, small, basal thinning flake. The latter has

modifications in the fracture of the quartz crystals, and micropolishing in the first stages of formation associated with striations and small pits suggests that this projectile point was hafted (Fig. 3B). The orthoquartzite side scraper fragment (FCS.CLA.183) is made from a large flake without cortex. It has two working edges with unifacial and marginal retouches (Fig. 3C). This tool is completely modified by sedimentary abrasion and soil sheen that render any polishing unrecognizable (28).

Excluding micromammals, 282 faunal bones were recovered. One individual each of three extinct megafauna taxa was identified: a giant ground sloth (*M. americanum*) and two glyptodonts (*Neosclerocalyptus* sp. and *Doedicurus* sp.). Giant ground sloth fossils were, by far, the most abundant [79 elements, number of identified specimens (NISP) = 108], and all the anatomical elements of the body were present, including 102 dermal bones assigned to *M. americanum* (table S1). One *Neosclerocalyptus* sp. humerus and one partial *Doedicurus* sp. femur were also recovered (table S1). Modern species are represented by a few remains of Patagonian hare (*Dolichotis patagonum*), vizcacha (*Lagostomus maximus*), dwarf armadillo (*Zaedyus pichiy*), peccary (*Tayassu* sp.), fox (*Lycalopex* sp.), bird (Rheidae), and artiodactyls (Camelidae) (table S2). A significant number of smaller vertebrates were also recovered: *Reithrodon auritus*, *Ctenomys* sp., *Akodon* cf. *Akodon azarae*, and *Galea leucoblephara* (20, 29). With the exception
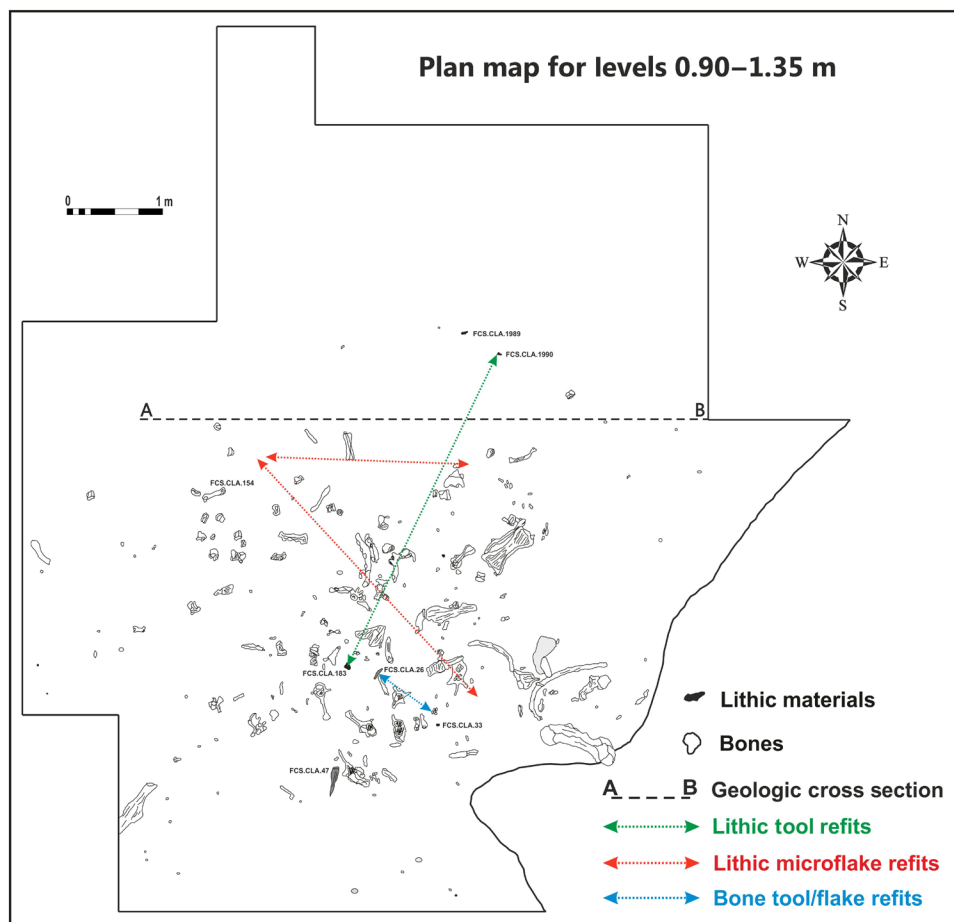
Fig. 2. Plan map of the Campo Laborde excavation site. Distribution of complete and fragmentary bones and lithic tools. Shaded drawings (black) indicate lithic materials (FCS.CLA.33, FCS.CLA.183, FCS.CLA.1989, and FCS.CLA.1990). Red and green dashed lines show lithic refits. Sample dated in this paper (FCS.CLA.154). A-B black line indicates geologic cross section (see Fig. 4 and fig. S5).
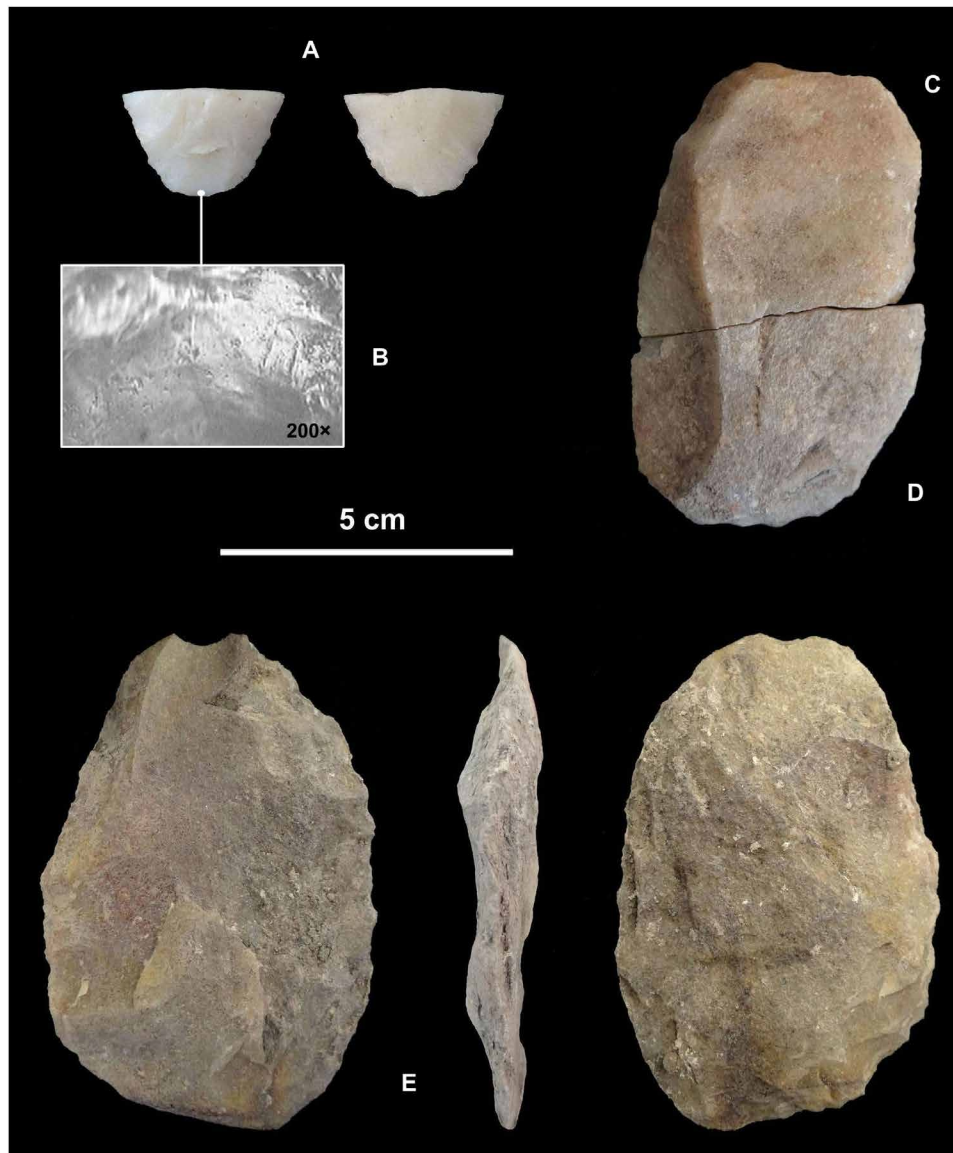
Fig. 3. Lithic tools found at Campo Laborde site. (**A**) Lanceolate bifacial projectile point stem (FCS.CLA.33). (**B**) Striations and small pits related with hafted micropolishing (×200 magnification). (**C**) Distal half of a broken side scraper (FCS.CLA.183). (**D**) Proximal half of a broken side scraper (FCS.CLA.1990). (**E**) Biface (FCS.CLA.1989). [Photo credit: Pablo Messineo. INCUAPA-CONICET, Facultad de Ciencias Sociales (UNICEN)].

of the giant ground sloth and the Patagonian hare (see cultural modification below), all other modern and small vertebrates species are interpreted as the result of incremental accumulation of fossil bones ("bone rain") that occur at the site due to natural deaths (eto-ecological processes) and owl activity (*29*) that postdate human-*Megatherium* interaction. In relation to the rest of the other megamammal species (*Neosclerocalyptus* sp. and *Doedicurus* sp.), it is difficult to interpret their incorporation into the deposit as a result of human activity since they are only represented by a single bone each (absence of any evidence of a human selective pattern) and they do not show any trace of human action on bones (cut marks, impact points, anthropic fractures, or burning).

In contrast, in addition to the close stratigraphic, vertical and horizontal association with lithics (Fig. 2 and fig. S2), other evidence supports the butchering and processing of *M. americanum* and *D. patagonum.* Evidence of butchering included stone tool modifi-

cations on an *M. americanum* rib (FCS.CLA.9) and a *D. patagonum* tibia (FCS.CLA.227), as well as flakes and helical fractured bones of megafauna taxa caused by human agency (fig. S3A). We made all diagnoses and identifications on the original specimens under a Leica Stereo Zoom S6D Trinocular stereoscopic microscope with magnifications ranging from 6.3 to 40× under adjustable incident light and with a digital Leica DMC 4500 camera.

Cut marks on the right rib of *M. americanum* are located on the interior surface. They represent four areas of marks with a transverse orientation to the rib axis (Fig. 4). This element shows unambiguous stone tool cut marks that are perpendicular to the cortical surface, straight V-shaped in cross section, and with internal microstriations, two of them showing multiple parallel marks (Fig. 4). We infer that these marks are associated with defleshing the animal. Cut marks on a *D. patagonum* tibia are located on the posterior surface of this

Fig. 4. Cut marks on *M. americanum* rib (FCS.CLA.9). [Photo credit: Pablo Messineo. INCUAPA-CONICET, Facultad de Ciencias Sociales (UNICEN)].

element and have a length of ~1 cm, with an oblique/transverse orientation, generally parallel to the axial axis of the bone (fig. S4). These cut marks were interpreted as a result of activities related to the skinning the animal (*29*).

In addition, two bone tools were made from megamammal ribs. One of them corresponds to the right distal end of *M. americanum* rib (FCS.CLA.47), which is a fracture-based utilitarian bone tool and has a rounded and polished fracture edge (fig. S3B). We solely placed these traces on the end section of the fracture edge (fig. S3C), whereas adjoining segments of the fracture edge and the rest of the rib do not present any type of bone modifications (i.e., abraded, smoothed, and polished). The second bone tool is a fragment of a rib (FCS.CLA.184) from an unidentified megafaunal species (same size of *Megatherium*) that has, at least, five negative flaking scars along the external compact bone produced during the manufacture of the tool (fig. S3D). One bone flake (FCS.CLA.26) was refitted onto one of these negative scars (fig. S3E). The bone tool and flake were separated by ~0.75 m horizontally (Fig. 2). The distal end edge of this bone is rounded and polished with parallel striations and microflaking on the external cortical surface (fig. S3F). This is probably related to its use. In the use-wear analysis, the wear polish was interpreted as the result of contact between the bone tool and a hard material. It is important to remark that no other bones in the collection show evidence of abrasion or polishing, not even in a lower degree (as happens occasionally in swamp environments). These observations support the human manufacture of the two bone tools (*28*).

Geologic studies identified stratigraphic units typical of the Late Pleistocene-Holocene Pampas (Fig. 5 and fig. S5). In the lower section of the profile (~1.30 to 1.35 m BGL), lacustrine sediments corresponding to the Luján Formation (*30*) are present. Most of the

archeological deposit (i.e., bones and lithics) was located from approximately 0.95 to 1.30 m BGL in stratum 1. This paleoswamp unit rested unconformably on Guerrero Member sediments and consisted of alternating layers of silty clays and sandy muds whose deposition was punctuated by pedogenesis (Fig. 5 and fig. S5). We excavated small numbers of microflakes (*n* = 25) and small bone fragments in an overlying paleosoil, 3Ab3, between 0.85 to 0.95 m BGL (fig. S6). These two units are located in a transition between the Río Salado and Guerrero Members (*20*, *30*). Above the archeological deposits are two additional buried soils; the stratigraphic sequence is capped by the modern soil (A). We recovered no archeological evidence from sediments above 0.85 cm BGL (Fig. 5 and fig. S5). The lithics are directly associated with the sloth's stratigraphic position and occur from 0.85 to 1.35 cm BGL, mainly in stratum 1 (figs. S5 and S6). The scarce materials found in the Guerrero Member and in the paleosoil 3Ab3 are due to the vertical migration of microflakes and small nonidentifiable bones from the stratum 1 (3ACb3 and 3AC3; see refitting among lithic materials).

The chronology of Campo Laborde has been difficult to establish due to extreme degradation and loss of bone organic matter and the bones' severe humate contamination. Initially, only 7 of 12 bones had detectable collagen (table S3). *M. americanum* fossils containing collagen yielded ages ranging from 6740 ± 480 ^{14}C years BP (AA-71667) to 9730 ± 290 ^{14}C years BP (AA-71665). We obtained two soil organic matter samples from the northern profile of the site. One of the samples came from paleosoil 3Ab3 and gave a date of 7960 ± 100 ^{14}C years BP (LP-1983). The second sample was taken from stratum 1, the paleoswamp where there was the highest proportion of bones and stone materials and provided an age of 8090 ± 190 ^{14}C years BP (LP-2003). These results should be taken with caution because dates obtained from soil organic matter must be considered
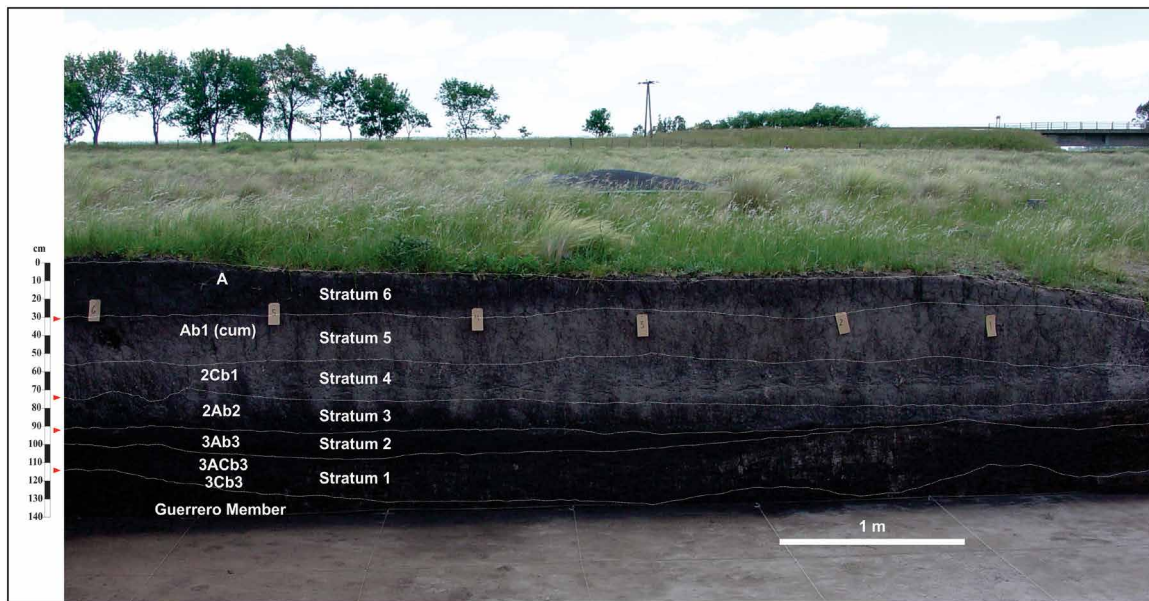
Fig. 5. Stratigraphy of the Campo Laborde site. [Photo credit: Pablo Messineo. INCUAPA-CONICET, Facultad de Ciencias Sociales (UNICEN)].

minimum soil ages and do not date the time of human occupation. Since this group of ages roughly dated this component between ~9700 and 6750 ^{14}C years BP, Campo Laborde was interpreted as an Early Holocene giant ground sloth procurement site along the border of an ancient swamp, where megafauna were killed and butchered (*20*, *21*). Although the possibility that the giant ground sloth was scavenged by humans cannot be ruled out (*31*, *32*), we believe that the sloth would have been hunted on the basis of the location of the event (driving prey into a swamp is a frequent hunting strategy) and the finding of a the broken bifacial projectile point that could be interpreted as one of the hunting tools (*27*).

Excavations in 2016 and 2017 (Fig. 2 and fig. S7A) yielded a taxonomically indeterminate rib fragment, 2 *M. americanum* metapodials (fig. S7B), 1 *Lama guanicoe* cervical vertebra (tables S1 and S2), 2 orthoquartzite tools (Fig. 3, D and E, and fig. S7, C and D), and 58 microflakes and debitage made from orthoquartzite, chert, silicified dolomite, and quartz. All the lithic materials and bone remains were found in stratum 1, the paleoswamp, between 0.95 and 1.30 m BGL. One of the tools is a knife manufactured on a biface (FCS.CLA.1989; 81.6 cm by 55.8 cm by 15.3 cm); one of the convex edges has been retouched and has an angle of ~40° to 50°, which makes it suitable for cutting activities (Fig. 3E). The other tool is the proximal half of a broken side scraper (FCS.CLA.1990) that refits with the other distal half (FCS.CLA.183) found ~3.5 m away in 2003 (Figs. 2 and 3, C and D). The edge of the distal-half side scraper was resharpened after breaking (Fig. 3C), indicating that the tool was broken during use and that one-half was repaired and used again. In 2003, four silicified dolomite microflakes that came from different grids and levels also refitted (Fig. 2). One of the refits was between proximal (FCS.CLA.238) and distal (FCS.CLA.251) flakes that were separated by ~2 m horizontally (Fig. 2). The other refit connects proximal (FCS.CLA.239) and medial (FCS.CLA.242) flakes separated by ~3 m horizontally (Fig. 2). In this last refitting, one fragment come from the level 1.30 to 1.35 m BGL (in the limit between the Guerrero Member and the paleoswamp) and the other piece come from the level 1.20

to 1.25 m BGL (stratum 1), supporting the conclusion that the lithic material in Campo Laborde is associated with the paleoswamp and the small quantity of microflakes in the Guerrero Member and in the stratum 2 (paleosoil 3Ab3) correspond to vertically dislocated materials. This vertical migration of microflakes may be the result of the depositional environment (lentic environment of alluvial plain margin) and pedogenic processes that subsequently affect the deposit. Likewise, the presence of few burrows and a small grouping of bones (*Ctenomys* sp.) in a limited sector of the site supports the action of fossorial animals and could explain the migration of microflakes downward and upward into the Guerrero Member and the stratum 2.

2016–2017 AMS ^{14}C DATING PROGRAM

Accurate and precise radiocarbon chronologies are the foundation for studying Late Pleistocene megamammal extinction times and rates and for assessing what degree of temporal overlap exists between extinct taxa and humans. Once initial stratigraphic association is shown between megamammal fossils and human-manufactured lithic or bone artifacts, and these associations are determined taphonomically valid, the geologic age of these sites is determined by directly dating bones of the extinct mammals and bone tools. Indirect dating of physically associated macroflora, microfauna, molluscs, nonextinct mammal taxa, or organic matter from enclosing sediments or soils is not acceptable.

Excepting bones from tar seeps, fossil bones from Campo Laborde and similar localities are the most difficult to radiocarbon date accurately. Campo Laborde fossils have zero to low quantities of collagen, the collagen is poorly preserved chemically and is difficult to extract, and the protein (collagen) is heavily contaminated with sedimentary and soil organic matter, usually occurring as humates (fulvic acids, humic acids, and humins). The single most intransigent chemical problem to overcome is the covalent bonding of humates to collagen, which occurs through the Maillard reaction (*33*). Separating

humates from collagen and isolating indigenous collagen and its amino acids require chemical pretreatments not commonly used by radiocarbon laboratories.

Humate contamination cannot be overcome by using standard bone collagen preparation techniques (e.g., decalcification, alkali leaching, gelatinization, or ultrafiltration). During burial, the Maillard reaction covalently binds humic and fulvic acids to proteins (17, 33), resulting in very dark brown to light yellowish brown collagen (34). Although alkali treatment extracts some humates, and gelatinization removes other, nonbound humates, covalently bound humic and fulvic acids can only be separated from collagen by breaking the collagen-humate bounds by hydrolyzing the collagen in 6 M HCl for 24 hours at 110°C (35). The resulting hydrolyzate contains free, cationic amino acid hydrochlorides and weakly charged to uncharged fulvic acids. The collagen's amino acids are isolated for ^{14}C dating by passing the hydrolyzate through hydrophobic XAD-2 resin, which binds to the fulvic acids and allows the amino acids to pass through XAD-2 resin.

Low collagen content per se is not a hindrance to ^{14}C dating fossil bones or teeth. One concern is that larger masses of bone are needed to compensate for low weight percentages of collagen (e.g., needing 5 g of bone instead of 0.1 g). A greater problem with low protein content is the remaining collagen has undergone increasingly more diagenesis, which decreases the protein's stability during HCl decalcification and KOH treatment and decreases the collagen's solubility during gelatinization. The result is that less protein is recoverable, and although the bone initially contained marginal amounts of collagen, no collagen may ultimately be recoverable.

Previous ^{14}C dating of extinct fauna from Campo Laborde (table S3) yielded Holocene ages ranging from 6740 ± 480 (AA-71667) to 9730 ± 290 ^{14}C years BP (AA-71665). We obtained these ages using three different chemical fractions: (i) acid-base-acid purified collagen (alkali-extracted decalcified collagen), (ii) gelatin, and (iii) ultrafiltered (> 30 kDa) gelatin (table S3 and Materials and Methods).

In 2016–2017, only 1 of 10 bones processed from Campo Laborde contained collagen. The one successful specimen was an *M. americanum* Metacarpal V (FCS.CLA.154; Fig. 2) that was first dated in 2007 as 9730 ± 290 ^{14}C years BP (AA-71665; table S3) and was redated. AMS ^{14}C measurements for this paper used XAD-2 resin purification to date total amino acids from hydrolyzed collagen and fulvic acids separated from the collagen hydrolyzate (Table 1, table S4, and Materials and Methods). XAD purification followed Stafford *et al.* (35) and Stafford (34) and comprised decalcification in HCl, extraction with KOH, gelatinization and filtering through 0.45-µm membranes, 6 M HCl hydrolysis, and passing the hydrolyzate through XAD-2 resin. Fulvic acids bound to the XAD resin were eluted by washing the resin with 0.05 M HCl to remove excess acid, eluting the fulvic acids with 0.05 M NaOH, drying the liquid under vacuum, and finally, acidifying the fulvic acids solution with 1 M HCl. AMS ^{14}C measurements on XAD hydrolyzates produced three radiocarbon ages (RC years ± 1 SD) for the Metacarpal V: 10,570 ± 170 ^{14}C years BP (CAMS-171851), 10,655 ± 35 ^{14}C years BP (CAMS-171852), and 10,690 ± 380 ^{14}C years BP (CAMS-171861; Table 1). AMS ^{14}C measurements (fraction modern or Fm) on fulvic acids solution represent an integration of all ages of fulvic acids that accumulated in the bone since its deposition. While the average Fm value for the three XAD dates was 0.2660 ± 0.0078, the fulvic acids had a higher (more modern) averaged Fm = 0.3238 ± 0.0099. Calculated "ages" for the fulvic acids are given to demonstrate that fulvic acids contain more

[14]C than the collagen and cause more recent (Holocene) ages when non-XAD chemistry is used to date the bones (Table 1 and table S4).

We conclude that humates remaining in collagen caused the previous Campo Laborde bones to date younger than their actual age and that only XAD purification chemistry is acceptable. While well-preserved collagen with no-to-negligible humates can sometimes be dated accurately using either ultrafiltered or 0.45-µm filtered gelatin (34, 36), both filtration methods and lesser purity fractions as decalcified collagen and alkali-extracted collagen will produce erroneous ^{14}C dates.

A geologic profile 20 m upstream from Campo Laborde was studied (37), with paleosoil 3Ab3 being reinterpreted as a black mat (highly organic marsh deposit). The study produced a date of 5680 ± 40 ^{14}C years BP (Beta-254925) on organic material from the black mat and a date of 8550 ± 50 ^{14}C years BP (Beta-254924) from a biogenic cavity fill below the paleoswamp (where we recovered most of the archeological evidence). This cavity fill was interpreted as an "intrusion of younger organic matter from overlying early Holocene marshes" (37). In addition to the ^{14}C dates, an Optically Stimulated Luminescence age of 12,120 ± 2120 years BP (X-3565) was measured for the paleoswamp. Last, *Succinea* sp. shells were dated as 10,620 ± 60 ^{14}C years BP (Beta-254926) and 10,420 ± 60 ^{14}C years BP [Beta-254928 (35)]. On the basis of these results, Toledo and Schewenninger (37) concluded that the bone samples from several Pampean archeological sites (e.g., La Moderna and Paso Otero 5) had been contaminated by younger organic matter and that Campo Laborde "…appear(s) to have a terminal Pleistocene age (12-14 ka CAL BP? and not a basal Holocene age as previously proposed, …)".

DISCUSSION

The interpretation of Campo Laborde as a kill (or procurement) and butchering site makes it difficult to discuss the broader subsistence pattern during Late Pleistocene times in the Pampas (23, 38) because this type of site can bias the interpretations about the subsistence strategies as a whole. However, on the basis of the evidence from other sites, the role of megafauna appears to have greater importance in the Pampas during this period in comparison with other regions of South America (38). The presence of the orthoquartzite stem allows a comparison with the other projectile points from the Pampas. The main projectile point type in the region is the Fishtail point, which has been dated between ~11,800 and 10,000 ^{14}C years BP (39–42), although the only site in the region with a clear association between this point type and extinct megamammals is Paso Otero 5 (43), which dates between 10,440 ± 100 ^{14}C years BP and 9560 ± 50 ^{14}C years BP. While Fishtail points are the most abundant in the Pampas, other Late Pleistocene projectile types have been recorded in the region (44) and in the Southern Cone (45). Among them, Tigre points in the Pampas of Uruguay show a wide stem with a convex base and have been dated between ~10,420 and 9730 ^{14}C years BP (44). However, no Tigre points have been found in the Pampas of Argentina. In any case, the stem found in Campo Laborde (with a similar concave base but different in dimensions and technological features) suggests that, around 10,650 ^{14}C years BP, at least two projectile point models were used to hunt Pleistocene megamammals in the Pampas of Argentina. Moreover, the bifacial knife of Campo Laborde also confirms the use of this technology in the Pampas at the end of the Pleistocene and shows similarities with other comparable artifacts (42, 44).

Table 1. AMS radiocarbon measurements for Campo Laborde *M. americanum* Metacarpal V (FCS.CLA.154) and humates separated during chemical pretreatment. Accepted age is 10,655 ± 35 ^{14}C years BP (CAMS-171852) due to having the highest mass bone (3.058 g) and lowest SD. NA, not available; C.I., confidence interval.

AMS Lab no.	Chemical fraction dated	Bone processed (g)	Carbon dated (µg)	Fm ± SD	^{14}C date ± 1 SD RC years BP	CAL BP (2σ) 95.4% C.I. (*46*)
Original University of Arizona analysis						
AA-71665	Gelatin	—	22	0.298 ± 0.011	9730 ± 290	10,250–11,982
CAMS bone dates						
CAMS-171861	XAD KOH-extracted decalcified collagen	1.025	40	0.2642 ± 0.0122	10,690 ± 380	11,304–13,207
CAMS-171873	Fulvic acids eluted from CAMS-171861 XAD resin	—	165	0.3397 ± 0.0030	8670 ± 80	NA
CAMS-171851	XAD decalcified collagen	1.137	90	0.2684 ± 0.0056	10,570 ± 170	11,924–12,732
CAMS-171875	Fulvic acids eluted from CAMS-171851 XAD resin	—	30	0.2983 ± 0.0167	9720 ± 450	NA
CAMS-171852	XAD KOH-extracted decalcified collagen	3.058	410	0.2654 ± 0.0010	10,655 ± 35	12,547–12,677
CAMS-171874	Fulvic acids eluted from CAMS-171852 XAD resin	—	165	0.3335 ± 0.0021	8670 ± 80	NA

The Pampas region has consistently produced younger last appearance dates for extinct megafauna than other regions of South America (*9*), leading some researchers to propose that it served as a refugium during the Late Pleistocene (*7*, *15*). Pampas region sites with published Early Holocene radiocarbon dates on extinct megafauna include Arroyo Seco 2 (*7*, *10*), La Moderna (*7*, *19*), Paso Otero 4 (*22*), Arroyo Tapalqué (*10*), Centinela del Mar (*10*), and Río Cuarto (*25*). Many of these Holocene dates have been rejected by authors due to diagenetic concerns or failure to replicate dates or are otherwise suspect because the material dated is considered less reliable than bone collagen (e.g., tooth enamel bioapatite carbonate). Notably, none of these dates used amino acid–based methods, except some of the Arroyo Seco 2 dates (*18*), and therefore, this study raises the possibility that the Holocene ^{14}C ages may be due to contamination by fulvic acids and other exogenous compounds that cannot be completely removed by traditional radiocarbon preparation methods. This contamination may be a particular problem in the Pampas, as compared with other parts of South America, because the open-air, fluvial, and lacustrine deposits typical of the region both produce low collagen yields through leaching and offer ample opportunity for plant- and animal-based humates to penetrate bones and bind with collagen.

cass. The refitting of side scraper fragments and microflakes supports the stratigraphic integrity of the deposit and that butchering activities and resharpening of artifacts occurred at the site. Microwear analysis on the broken projectile point stem indicates that it was hafted.

The new ^{14}C measurements solidly date the killing and exploitation of the giant ground sloth to the Late Pleistocene. These new dates do not support extinct megamammals surviving into the Holocene at Campo Laborde and call into question Holocene survival of megafauna at most, if not all, Pampas localities. Certainly, more radiocarbon analyses using amino acid–based methods are necessary in sites such as La Moderna to test the supposedly Holocene age of the extinct megamammals in these sites.

Campo Laborde is the only confirmed giant ground sloth kill site in the Americas. New dating also reduces the time span between the arrival of humans and the extinction of the megamammals in the Pampas of Argentina in ~2000 years. Both of these results support previous proposals (*3*, *7*) on the contribution of human impact in the extinction process of the South American megafauna. The Pampas data are evidence that some extinct species (e.g., *Megatherium*, *Equus*, and *Doedicurus*) were exploited by people, probably with a low level of predation, over at least two millennia, before their extinction.

CONCLUSIONS

The recent excavations and new ^{14}C dates support Campo Laborde being a kill and butchering site bordering a Late Pleistocene swamp. The lithic artifacts found around and within the giant ground sloth bone concentration suggest that hunters knapped directly around the car-

MATERIALS AND METHODS
Radiocarbon sample preparation
The following summaries describe what chemical pretreatments were performed by each laboratory. The University of Arizona AMS Lab processed dates labeled as AA−. Dates shown as CAMS− were

chemically prepared and combusted by E.L.L. and were graphitized and AMS ^{14}C–dated at the LLNL Center for Accelerator Mass Spectrometry, California.

AA-55117, AA-55118, and AA-55119

Bone samples were demineralized in 0.25 M HCl, and the acid-insoluble fraction was extracted with deionized (DI) water (pH 2) at 60°C. The hot water soluble fraction was dried and combusted to yield CO_2 for graphitization.

AA-71665 and AA-71667

Bone samples were demineralized in dilute HCl, leached with NaOH, and acidified with dilute HCl using a continuous flow Acid-Base-Acid (ABA) extraction system to yield the ABA-treated bone fraction used for combustion and dating.

CAMS-155863

Approximately 200 mg of uncrushed, mechanically cleaned *M. americanum* rib bone (FCS.CLA.9) was decalcified in 0.25 M HCl at 4°C for 72 hours, replacing HCl daily, until the sample softened (the sample never attained the fully soft, spongy texture characteristic of demineralized collagen). The sample was then gelatinized in 0.1 M HCl at 58°C for 16 hours, after which the solution was filtered through a Whatman quartz fiber filter with vacuum suction and then ultrafiltered through 30-kDa Centriprep centrifugal filters that had been prerinsed via centrifugation four times in Milli-Q purified water. The ultrafiltered collagen was freeze-dried and combusted at 850°C for 12 hours in quartz tubes containing copper oxide (CuO) and silver (Ag). The resulting CO_2 was purified and graphitized for AMS ^{14}C measurement.

CAMS-171851, CAMS-171852, and CAMS-171861

Approximately 1 g of bone for samples CAMS-171851 and CAMS-171861 and 3 g for CAMS-171852 were removed from *M. americanum* Metacarpal V (FCS.CLA.154) and were mechanically cleaned with a Dremel tool. Bone fragments approximately 5 to 10 mm long were decalcified at 4°C in 0.2 to 0.5 M HCl for up to 35 days. Decalcification was considered complete when (i) CO_2 effervescence had ceased, (ii) the resulting collagen had a translucent appearance and spongy texture, and (iii) no calcium phosphate density gradient was apparent after the sample had been stationary for several hours in fresh HCl. CAMS-171861 was subsequently alkali-extracted with 0.1 M KOH for 2 days at 38°C.

All decalcified collagen samples were rinsed in DI water and placed in sealed tubes with 6 M HCl on a heating block at 110°C for 22 hours to hydrolyze the collagen. Heating in strong HCl hydrolyzes the protein's peptide bonds to form free amino acids, releases humates bound to the collagen through the Maillard reaction, and causes other humate-related compounds to precipitate. The amino acids are cationic in strong acid, while the hydroxyl and carboxyl groups of the fulvic acids are fully protonated, making them neutral molecules that strongly bind to the nonpolar XAD-2 resin. The hydrolyzates were passed through XAD-2 columns containing approximately 2 ml of Restek Ultra-Clean XAD-2 resin retained between two 20-μm Restek SPE frits; each column was fitted at the bottom with a 0.45-μm Restek SPE filter cartridge. The XAD-filtered hydrolyzates were evaporated in a vortex evaporator, and between 1 and 6 mg of hydrolyzed collagen, were combusted in sealed quartz tubes containing copper oxide (CuO) and silver (Ag).

CAMS-171873, CAMS-171874, and CAMS-171875

Following the XAD-2 purification of the amino acid hydrolyzates for samples CAMS-171851, CAMS-171852, and CAMS-171861, the resin columns were washed with DI water (pH 8) to remove

excess HCl. Fulvic acids bound to the resin were eluted using a few tens of microliters of 0.1 M KOH; the elute was acidified with HCl, dried, and combusted in sealed quartz tubes containing copper oxide (CuO) and silver (Ag). All CO_2 resulting from the combustions was graphitized, and targets were analyzed by accelerator mass spectrometry.

SUPPLEMENTARY MATERIALS

Supplementary material for this article is available at http://advances.sciencemag.org/cgi/content/full/5/3/eaau4546/DC1

Fig. S1. View of *M. americanum* bones (ribs and vertebrae) and lithic tool (red arrow) recovered in 2003.
Fig. S2. Horizontal lithic distribution in Campo Laborde.
Fig. S3. Bone tools and flakes.
Fig. S4. Cut marks on *D. patagonum* tibia (FCS.CLA.227).
Fig. S5. Stratigraphic scheme of the Campo Laborde site.
Fig. S6. Vertical lithic distribution at Campo Laborde site.
Fig. S7. Bones and lithics exposed during new excavation.
Table S1. Stratigraphic and anatomical data for skeletal elements of giant ground sloth (*M. americanum*) and glyptodonts (*Neosclerocalyptus* sp. and *Doedicurus* sp.) recovered from Campo Laborde.
Table S2. Stratigraphic and anatomical data for skeletal elements (MNE) of modern fauna recovered from Campo Laborde.
Table S3. Previous AMS ^{14}C dates from Campo Laborde.
Table S4. AMS radiocarbon measurements for known-age samples and backgrounds.
References (*47*, *48*)

REFERENCES AND NOTES

1. A. D. Barnosky, P. L. Koch, R. S. Feranec, S. L. Wing, A. B. Shabel, Assessing the causes of late Pleistocene extinctions on the continents. *Science* **306**, 70–75 (2004).
2. P. L. Koch, A. D. Barnosky, Late Quaternary extinctions: State of the debate. *Annu. Rev. Ecol. Evol. S.* **37**, 215–250 (2006).
3. A. L. Cione, E. P. Tonni, L. Soibelzon, Did humans cause the Late Pleistocene-Early Holocene mammalian extinctions in South America in a context of shrinking open areas? in *American Megafaunal Extinctions at the End of the Pleistocene*, G. Haynes, Ed. (Springer, 2009), pp. 125–144.
4. N. A. Villavicencio, E. L. Lindsey, F. M. Martin, L. A. Borrero, P. I. Moreno, C. R. Marshall, A. D. Barnosky, Combination of humans, climate, and vegetation change triggered Late Quaternary megafauna extinction in the Última Esperanza region, southern Patagonia, Chile. *Ecography* **39**, 125–140 (2016).
5. W. J. Ripple, B. V. Van Valkenburgh, Linking top-down forces to the Pleistocene megafaunal extinctions. *Bioscience* **60**, 516–526 (2010).
6. A. Goldberg, A. M. Mychajliw, E. A. Hadly, Post-invasion demography of prehistoric humans in South America. *Nature* **532**, 232–235 (2016).
7. G. G. Politis, J. L. Prado, R. P. Beukens, The human impact in Pleistocene-Holocene extinctions in South America. The Pampean case, in *Ancient Peoples and Landscapes*, E. Johnson, Ed. (Museum of Texas Tech University, 1995), pp.187–205.
8. L. A. Borrero, The elusive evidence: The archeological record of the South American extinct megafauna, in *American Megafaunal Extinctions at the End of the Pleistocene*, G. Haynes, Ed. (Springer, 2009), pp. 145–168.
9. A. D. Barnosky, E. L. Lindsey, Timing of Quaternary megafaunal extinction in South America in relation to human arrival and climate change. *Quat. Int.* **217**, 10–29 (2010).
10. J. L. Prado, C. Martinez-Maza, M. T. Alberdi, Megafauna extinction in South America: A new chronology for the Argentine Pampas. *Palaeogeogr. Palaeoclimatol. Palaeoecol.* **425**, 41–49 (2015).
11. C. N. Johnson, C. J. A. Bradshaw, A. Cooper, R. Gillespie, B. W. Brook, Rapid megafaunal extinction following human arrival throughout the New World. *Quat. Int.* **308–309**, 273–277 (2013).
12. A. Rozas-Davila, B. G. Valencia, M. B. Bush, The functional extinction of Andean megafauna. *Ecology* **97**, 2533–2539 (2016).
13. J. L. Metcalf, C. Turney, R. Barnett, F. Martin, S. C. Bray, J. T. Vilstrup, L. Orlando, R. Salas-Gismondi, D. Loponte, M. Medina, M. De Nigris, T. Civalero, P. M. Fernández, A. Gasco, V. Duran, K. L. Seymour, C. Otaola, A. Gil, R. Paunero, F. J. Prevosti, C. J. A. Bradshaw, J. C. Wheeler, L. Borrero, J. J. Austin, A. Cooper, Synergistic roles of climate warming and human occupation in Patagonian megafaunal extinctions during the Last Deglaciation. *Sci. Adv.* **2**, e1501682 (2016).
14. A. Hubbe, M. Hubbe, W. Neves, Early Holocene survival of megafauna in South America. *J. Biogeogr.* **34**, 1642–1646 (2007).
15. L. Miotti, E. P. Tonni, L. Marchionni, What happened when the Pleistocene megafauna became extinct? *Quat. Int.* **473**, 173–189 (2018).

16. M. L. Larson, M. Kornfeld, G. C. Frison, in *Hell Gap: A stratified Paleoindian Campsite at the Edge of the Rockies* (The University of Utah Press, 2009).

17. M. R. Waters, T. W. Stafford Jr., B. Kooyman, L. V. Hills, Late Pleistocene horse and camel hunting at the southern margin of the ice-free corridor: Reassessing the age of Wally's Beach, Canada. *Proc. Natl. Acad. Sci. U.S.A.* **112**, 4263–4267 (2015).

18. G. G. Politis, M. A. Gutiérrez, D. J. Rafuse, A. Blasi, The arrival of *Homo sapiens* into the Southern Cone at 14,000 years ago. *PLOS ONE* **11**, e0162870 (2016).

19. G. G. Politis, M. A. Gutiérrez, Gliptodontes y cazadores-recolectores de la Región Pampeana (Argentina). *Lat. Am. Antiq.* **9**, 111–134 (1998).

20. G. G. Politis, P. G. Messineo, The Campo Laborde site: New evidence for the Holocene survival of Pleistocene megafauna in the Argentine Pampas. *Quat. Int.* **191**, 98–114 (2008).

21. P. G. Messineo, G. G. Politis, New radiocarbon dates from the Campo Laborde site (Pampean Region, Argentina) support the Holocene survival of giant ground sloth and glyptodonts. *Curr. Res. Pleist.* **26**, 5–9 (2009).

22. G. Martínez, M. A. Gutiérrez, E. P. Tonni, Paleoenvironments and faunal extinctions: Analysis of the archaeological assemblages at the Paso Otero locality (Argentina) during the Late Pleistocene-Early Holocene. *Quat. Int.* **299**, 53–63 (2013).

23. G. Martínez, M. A. Gutiérrez, P. G. Messineo, C. A. Kaufmann, D. J. Rafuse, Subsistence strategies in Argentina during the late Pleistocene and early Holocene. *Quat. Sci. Rev.* **144**, 51–65 (2016).

24. G. G. Politis, M. A. Gutiérrez, C. Scabuzzo, in *Estado actual de las investigaciones en el sitio 2 de Arroyo Seco (Partido de Tres Arroyos, Provincia de Buenos Aires, Argentina)* (Serie monográfica 5, UNICEN-FACSO, 2014).

25. L. E. Cruz, M. S. Bargo, E. P. Tonni, A. J. Figini, Radiocarbon date on megafauna from the late Pleistocene-early Holocene of Córdoba province, Argentina: Stratigraphic and paleoclimatic significance. *Rev. Mex. Cienc. Geol.* **27**, 470–476 (2010).

26. G. G. Politis, E. Johnson, M. Gutiérrez, W. Hartwell, Survival of the Pleistocene fauna: New radiocarbon dates on organic sediments from La Moderna (Pampean Region, Argentina), in *Where the South Winds Blow: Ancient Evidence for Paleo South Americans*, L. Miotti, M. Salemme y N. Flegenheimer, Eds. (Center for the Study of the First Americans. Texas Univ. Press, 2003), pp. 45–50.

27. P. G. Messineo, Technological organization in hunting/scavenging and butchering sites of megamammals in the Pampa grassland (Argentina). *PaleoAmerica* **1**, 343–359 (2015).

28. P. G. Messineo, N. M. Pal, Techno-morphological and use-wear analysis in lithic and bone tools from Campo Laborde site (Pampean Region, Argentina). *Curr. Res. Pleist.* **28**, 115–117 (2011).

29. N. A. Scheifler, P. G. Messineo, U. F. J. Pardiñas, Los pequeños vertebrados del sitio arqueológico Campo Laborde: Procesos de incorporación y consideraciones paleoambientales. *Archaeofauna: Int. J. of Archaeozoology* **24**, 187–208 (2015).

30. F. Fidalgo, F. O. De Francesco, U. R. Colado, Geología superficial en las hojas Castelli, J. M. Cobo y Monasterio (Provincia de Buenos Aires). *Actas V Congreso Geológico Argentino* **4**, 27–39 (1973).

31. K. D. Lupo, Butchering marks and carcass acquisition strategies: Distinguishing hunting from scavenging in archaeological contexts. *J. Archaeol. Sci.* **21**, 827–837 (1994).

32. L. A. Borrero, F. M. Martin, Ground sloths and humans in southern Fuego-Patagonia: Taphonomy and archaeology. *World Archaeol.* **44**, 102–117 (2012).

33. H. Nursten, in *The Maillard Reaction: Chemistry, Biochemistry and Implications* (Royal Society of Chemistry, Cambridge, 2005).

34. T. W. Stafford Jr., Chronology of the Kennewick skeleton, Washington, in *The Scientific Investigation of an Ancient American Skeleton*, D. W. Owsley, R. L. Jantz, Eds. (Texas A&M Press, 2014), pp. 58–89.

35. T. W. Stafford Jr., K. Brendel, R. C. Duhamel, Radiocarbon, ^{13}C, and ^{15}N analysis of fossil bone: Removal of humates with XAD-2 resin. *Geochim. Cosmochim. Acta* **52**, 2257–2267 (1988).

36. T. Devièse, T. W. Stafford Jr., M. R. Waters, C. Wathen, D. Comeskey, L. Becerra-Valdivia, T. Higham, Increasing accuracy for the radiocarbon dating of sites occupied by the first Americans. *Quat. Sci. Rev.* **198**, 171–180 (2018).

37. M. J. Toledo, J. -L. Schewenninger, Black mats at the Pleistocene-Holocene transition in Pampean valleys: implications for ^{14}C dating, geoarchaeology and chronology of megafauna extinctions. *Actas del XIX Congreso Geológico Argentino*, S13-10 (Córdoba, 2014).

38. M. A. Gutiérrez, G. A. Martínez, Trends in the faunal human exploitation during the Late Pleistocene and Early Holocene in the Pampeana region (Argentina). *Quat. Int.* **191**, 53–68 (2008).

39. H. G. Nami, Arqueología del último milenio del Pleistoceno en el Cono Sur de Sudamérica: puntas de proyectil y observaciones sobre tecnología Paleoindia en el Nuevo Mundo in *Peuplement et Modalités d'Occupation de l'Amérique du Sul. L'Apport de la Technologie Lithiqué*, M. Farias, A. Lourdeau, Eds. (Prigonrieux, 2014), pp. 179–220.

40. G. F. Bonnat, D. L. Mazzanti, G. A. Martínez, Tecnología lítica y contexto geoarqueológico de la ocupación temprana del Sitio 2 de la localidad Arqueológica Amalia, provincia de Buenos Aires (Argentina). *Revista del Museo de Antropología* **8**, 21–32 (2015).

41. C. Weitzel, N. Flegenheimer, N. Mazzia, Assessing Fishtail points distribution in the southern Cone. *Quat. Int.* **473**, 161–172 (2018).

42. R. Suárez, G. Piñeiro, F. Barceló, Living on the river edge: The Tigre site (K-87) new data and implications for the initial colonization of the Uruguay River basin. *Quat. Int.* **473**, 242–260 (2018).

43. G. Martínez, M. A. Gutiérrez, Paso Otero 5: A summary of the interdisciplinary lines of evidence for reconstructing early human occupation and paleoenvironment in the Pampean region, Argentina, in *Peuplements et Préhistoire de l'Amérique*, D. Vialou, Ed. (Muséum National d'Histoire Naturelle. Departement de Prehistoire, U.M.R, Paris, 2011), pp. 271–284.

44. R. Suárez, The Paleoamerican occupation of the plains of Uruguay. *PaleoAmerica* **1**, 88–104 (2015).

45. C. Méndez Melgar, Terminal Pleistocene/early Holocene ^{14}C dates form archaeological sites in Chile: Critical chronological issues for the initial peopling of the region. *Quat. Int.* **301**, 60–73 (2013).

46. A. G. Hogg, Q. Hua, P. G. Blackwell, M. Niu, C. E. Buck, T. P. Guilderson, T. J. Heaton, J. G. Palmer, P. J. Reimer, R. W. Reimer, C. S. M. Turney, S. R. H. Zimmerman, SHCAL13 Southern hemisphere calibration, 0-50,000 years CAL BP. *Radiocarbon* **55**, 1889–1903 (2013).

47. G. G. Politis, E. Lindsey. Humans and Pleistocene megamammals in the Pampean Region, paper presented at the 77th Annual Meeting of the Society for American Archaeology. Memphis, Tennessee, 18 to 22 April 2012.

48. E. M. Scott, The Third International Radiocarbon Intercomparison (TIRI). *Radiocarbon* **45**, 293–328 (2003).

Science Advances

Campo Laborde: A Late Pleistocene giant ground sloth kill and butchering site in the Pampas

Gustavo G. Politis, Pablo G. Messineo, Thomas W. Stafford, Jr and Emily L. Lindsey

ARTICLE TOOLS	http://advances.sciencemag.org/content/5/3/eaau4546
SUPPLEMENTARY MATERIALS	http://advances.sciencemag.org/content/suppl/2019/03/04/5.3.eaau4546.DC1
REFERENCES	This article cites 36 articles, 3 of which you can access for free http://advances.sciencemag.org/content/5/3/eaau4546#BIBL
PERMISSIONS	http://www.sciencemag.org/help/reprints-and-permissions

Use of this article is subject to the Terms of Service

Supplementary Materials for

Campo Laborde: A Late Pleistocene giant ground sloth kill and butchering site in the Pampas

Gustavo G. Politis*, Pablo G. Messineo, Thomas W. Stafford Jr., Emily L. Lindsey

*Corresponding author. Email: gpolitis@fcnym.unlp.edu.ar

This PDF file includes:

Fig. S1. View of *M. americanum* bones (ribs and vertebrae) and lithic tool (red arrow) recovered in 2003. [Photo credit: Gustavo Politis. INCUAPA-CONICET, Facultad de Ciencias Sociales (UNICEN)].

Fig. S2. Horizontal lithic distribution in Campo Laborde.

Fig. S3. Bone tools and flakes. (**A**) Flakes on megafauna bone exhibiting dynamic impact features of wet bones (FCS.CLA.34; FCS.CLA.1492): cortical side exposing compact bone (left) and interior side with bulb of percussion that emanates out from the proximal area (right). (**B**) *Megatherium americanum* rib tool (FCS.CLA.47), the end-edge of the bone (**C**) is rounded and polished with parallel striations and microflaking. (**D**) Megamammal bone tool with negative flake scars exposing compact bone (FCS.CLA.184) produced during its manufacture. (**E**) Bone flake (FCS.CLA.26) refitting onto one of the negative scars (dotted white line in bone tool): cortical side exposing compact bone and interior (left) and interior side with bulb of percussion that emanates out from the proximal area (right). (**F**) The end-edge of the bone tool exhibits a rounded and smoothed surface. [Photo credit: Pablo Messineo. INCUAPA-CONICET, Facultad de Ciencias Sociales (UNICEN)].

Fig. S4. Cut marks on *D. patagonum* tibia (FCS.CLA.227). [Photo credit: Pablo

Messineo. INCUAPA-CONICET, Facultad de Ciencias Sociales (UNICEN)].
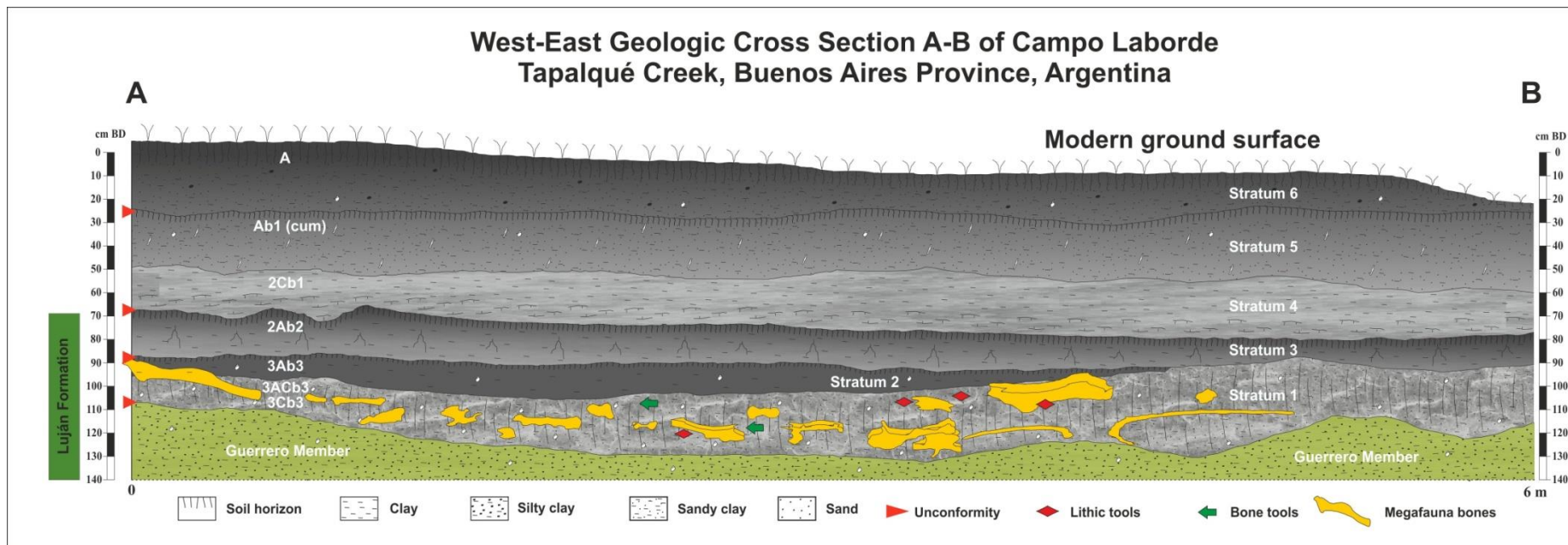
Fig. S5. Stratigraphic scheme of the Campo Laborde site. Distribution of *Megatherium americanum* bones (yellow), bone tools (green) and lithic tools (red) in the stratum 1.
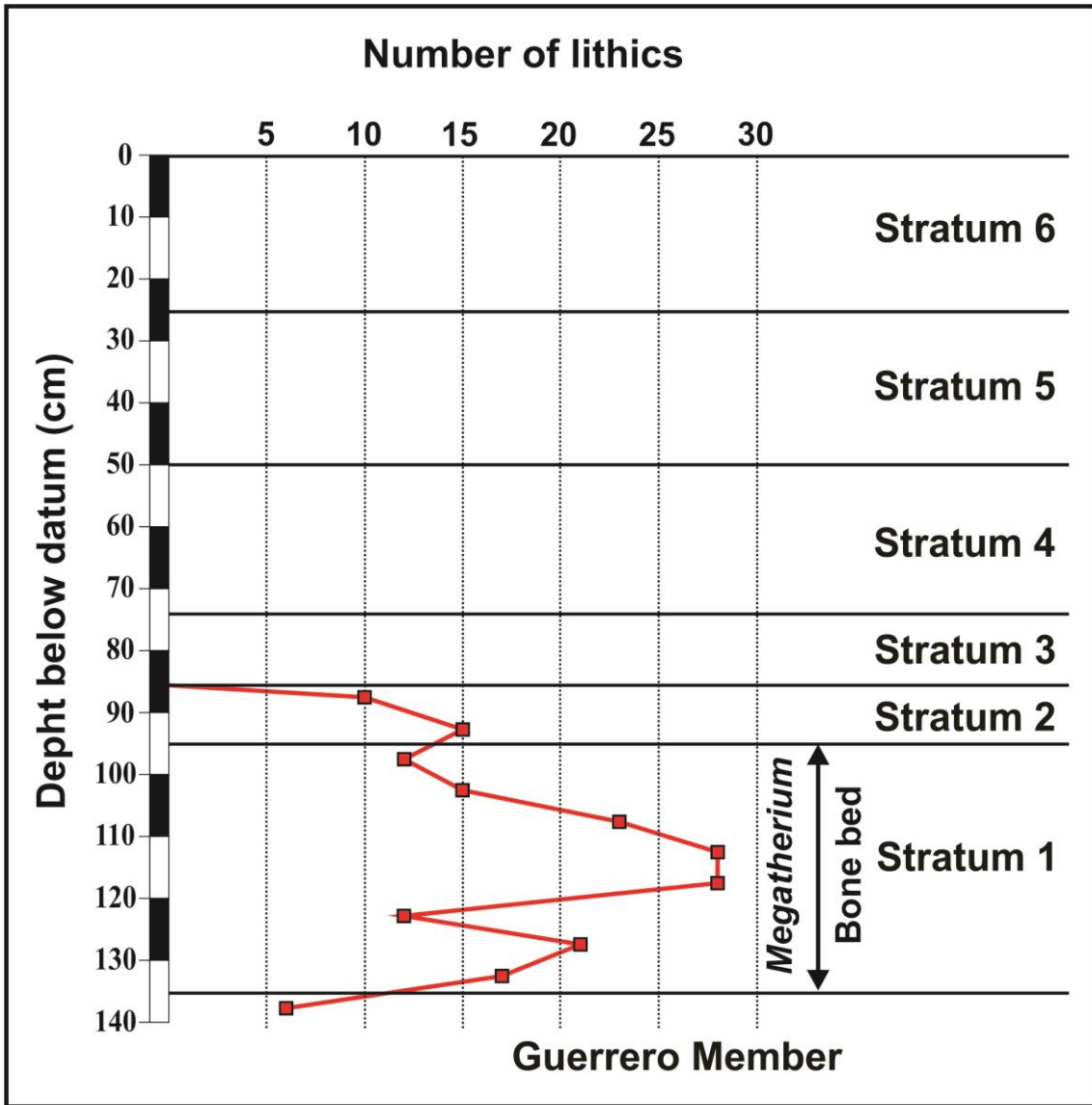
Fig. S6. Vertical lithic distribution at Campo Laborde site.
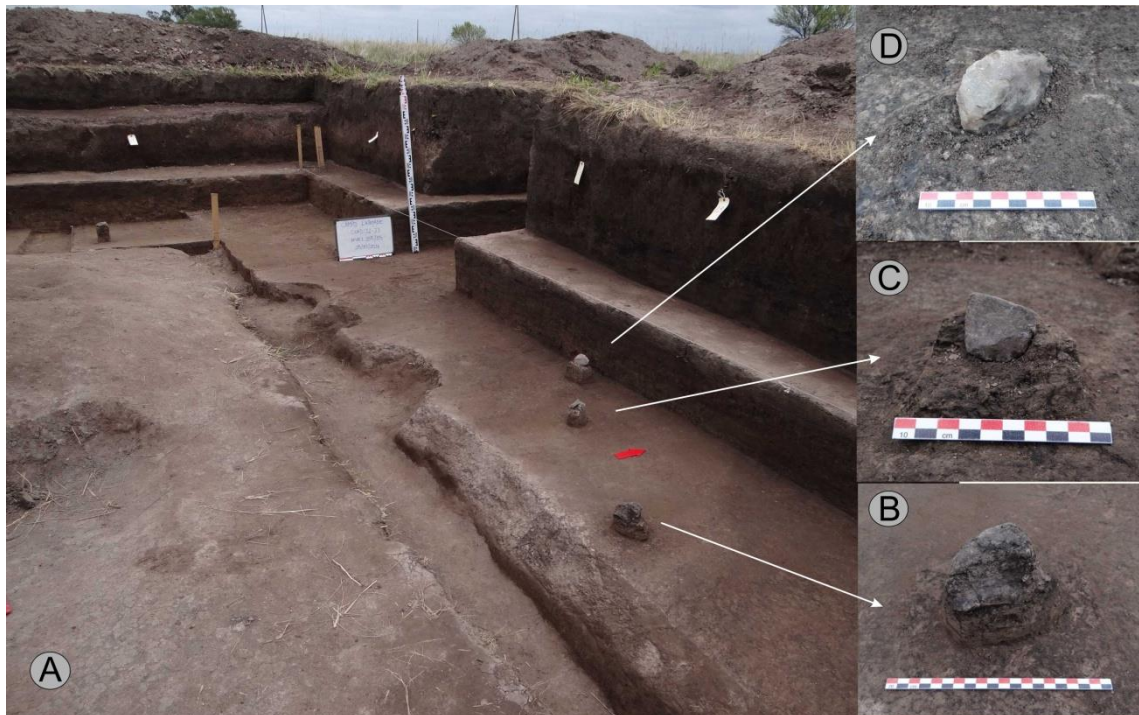
Fig. S7. Bones and lithics exposed during new excavation. (**A**) Oblique view of bones and lithic tools found in 2016. (**B**) *Megatherium americanum* autopodial bone (FCS.CLA.1992). (**C**) Proximal-haft of side scraper (FCS.CLA.1990). (**D**) Biface (FCS.CLA.1989). [Photo credit: Gustavo Politis. INCUAPA-CONICET, Facultad de Ciencias Sociales (UNICEN)].

Table S1. Stratigraphic and anatomical data for skeletal elements of giant ground sloth (*M. americanum*) and glyptodonts (*Neosclerocalyptus* sp. and *Doedicurus* sp.) recovered from Campo Laborde.

Catalogue number	Grid	North (meters)	West (meters)	Centimeters BGL	Element	NISP	MNE	Condition	Laterality
Megatherium americanum									
FCS.CLA.5	G2	1	0.04	121	Rib	1	-	Fragment	-
FCS.CLA.7	G2	0.61	0.35	126.5	Pelvis	1	1	Fragment	-
FCS.CLA.8	G2	0.79	0.86	137	Thoracic vertebra 6	1	1	Fragment	Axial
FCS.CLA.9	G2	0.65	0.88	137	Rib 8 or 9	1	1	Complete	Right
FCS.CLA.20	G3	0.5	0.45	100	Lumbar vertebra 4	1	1	Fragment	Axial
FCS.CLA.21	G3	0.45	0.23	103	Lumbar vertebra 3	1	1	Fragment	Axial
FCS.CLA.28	G3	0.60	1.02	116.5	Sternal segment portion Rib 8	1	1	Fragment	Left
FCS.CLA.35	F3	0.35	0.39	110.5	Sternal segment portion Rib 6	1	1	Fragment	Right
FCS.CLA.38	G3	0.05	1	109	Navicular (hindlimb)	1	1	Fragment	Right
FCS.CLA.39	E6	0	0.05	104.5	Radius	1	1	Complete	Right
FCS.CLA.46	F4	0.65	0.45	109	Thoracic vertebra	1	1	Fragment	Axial
FCS.CLA.47	F4	0.65	0.2	105.5	Rib 2 or 3	1	-	Fragment	Left
FCS.CLA.50	F4	0.6	0.78	108.5	Rib	1	-	Fragment	-
FCS.CLA.58	F4	0.65	0.63	107	Rib	1	-	Fragment	-
FCS.CLA.62	F6	0.45	0.59	101	Sternebra	1	1	Complete	Axial
FCS.CLA.70	G4	0.46	0	106	Sternal segment portion, Rib 3 or 4	1	-	Fragment	Right?
FCS.CLA.73	G4	0.4	0.18	107	Hyoid	1	1	Complete	Left?
FCS.CLA.74	G4	0.16	0.2	106.5	Sternal segment portion, Rib 3 or 4	1	1	Fragment	Right?
FCS.CLA.79	G5	0.88	0.01	112.5	Cervical vertebra 3	1	1	Fragment	Axial
FCS.CLA.81	G5	0.27	0.39	108	Hyoid	1	1	Complete	Right?
FCS.CLA.86	G6	0.13	0.22	110	Phalanx 2-II (forelimb)	1	1	Complete	Right
FCS.CLA.91	H2	0.3	0	109.5	Tibia	1	1	Complete	Left
FCS.CLA.92	H2	0.02	0.04	104	Metatarsal III	1	1	Fragment	Left
FCS.CLA.97	H2	0.05	0.1	106	Metatarsal III	1	-	Fragment	Left
FCS.CLA.99	H3	0.4	0.5	105	Sternal segment portion, Rib 4 or 5	2	1	Complete	Left

FCS.CLA.102	H3	0.88	0.42	101	Sternovertebra 2	1	1	Fragment	Axial
FCS.CLA.103	H3	0.98	0.4	101.5	Tibia-fibula	12	1	Fragment	Right
FCS.CLA.111	H3	0.23	0.82	108	Phalanx 3-V	1	1	Complete	-
FCS.CLA.115	H4	0.35	0.62	106.5	Sternal segment portion, Rib 8	1	-	Fragment	Left
FCS.CLA.118	H5	0.16	0.23	108	Magnum (forelimb)	1	1	Complete	Left
FCS.CLA.119	H5	0.74	0.36	110	Phalanx 3-V	1	1	Complete	-
FCS.CLA.120	H5	0.73	0.09	112.5	Ungual phalanx-II (forelimb)	1	1	Fragment	Right
FCS.CLA.122	H6	0.35	0.99	109	Scaphoid (forelimb)	1	1	Complete	Left
FCS.CLA.123	H6	0	0.98	110	Distal carpal external 4+5 (forelimb)	1	1	Complete	Left
FCS.CLA.124	H6	0.17	0.97	109	Phalanx 2-IV (forelimb)	1	1	Complete	Left
FCS.CLA.125	H6	0.17	0.85	113	Lunar (forelimb)	1	1	Complete	Left
FCS.CLA.132	I2	0.4	0.15	104	Sternal segment portion Rib 1	1	1	Fragment	Left
FCS.CLA.139	I3	0.61	0.43	110	Ungual phalanx-III (forelimb)	1	1	Complete	Right
FCS.CLA.140	I3	0.76	0.32	110	Cuboid (hindlimb)	1	1	Complete	Right
FCS.CLA.141	I3	0.74	0.23	110	Sesamoid	1	1	Complete	-
FCS.CLA.148	I4	0.8	0.08	108	Sternal segment portion Rib	1	-	Fragment	-
FCS.CLA.149	I5	0.31	0.14	1.08	Phalanx 1-II	1	1	Fragment	Right
FCS.CLA.150	I5	0.9	0.61	104.5	Magnum (forelimb)	1	1	Complete	Right
FCS.CLA.151	I5	0.59	0.84	108	Cubital (forelimb)	1	1	Complete	Right
FCS.CLA.153	I6	0.06	1	98	Sesamoid	1	1	Fragment	-
FCS.CLA.154	I6	0.75	0.98	106.5	Metacarpal V	1	1	Complete	Right
FCS.CLA.155	I6	0.73	0.8	107.5	Pisiform (forelimb)	1	1	Complete	Left
FCS.CLA.162	F4	0.14	0.87	117	Atlas	1	1	Complete	Axial
FCS.CLA.163	F4	0.47	0.53	113.5	Rib	1	-	Fragment	-
FCS.CLA.164	F4	0.13	0.55	121.5	Thoracic vertebra 4	1	1	Complete	Axial
FCS.CLA.165	F4	0.6	0.38	128	Thoracic vertebra 2	1	1	Complete	Axial
FCS.CLA.170	F5	0.12	0.43	132	Axis	1	1	Complete	Axial
FCS.CLA.174	G4	0.82	0.86	114.5	Cervical vertebra 6 or 7	1	1	Fragment	Axial
FCS.CLA.175	G4	0.35	0.01	114	Phalanx 1-2-III (forelimb)	1	1	Fragment	-
FCS.CLA.177	G4	0.75	0.08	121.5	Thoracic vertebra 3	1	1	Complete	Axial
FCS.CLA.178	G4	0.38	0.76	115.5	Rib 2 or 3	1	1	Fragment	Left
FCS.CLA.179	G4	0.7	0.7	111.5	Rib 2 or 3	1	-	Fragment	Left

FCS.CLA.185	G4	0.08	0.09	122	Sternebra	1	1	Complete	Axial
FCS.CLA.188	G5	0.74	0.67	113	Rib	1	-	Fragment	-
FCS.CLA.189	G5	0.35	0.66	119	Ectocuneiform (hindlimb)	1	1	Fragment	Right
FCS.CLA.192	H3	0.45	0.43	114	Metatarsal III	1	1	Fragment	Right
FCS.CLA.193	H3	0.62	0.64	117	Ectocuneiform (hindlimb)	1	1	Fragment	Left
FCS.CLA.194	H4	0.78	0.45	131	Cervical vertebra 5	1	1	Fragment	Axial
FCS.CLA.195	H4	0.2	0.74	116.5	Metacarpal II	1	1	Fragment	Right
FCS.CLA.196	H4	0.33	0.92	126.5	Thoracic vertebra 9 or 10	1	1	Fragment	Axial
FCS.CLA.197	H4	0.72	0.67	128	Cervical vertebra 4	1	1	Fragment	Axial
FCS.CLA.198	H4	0.9	0.5	124.5	Hyoid apparatus	2	1	Complete	Axial
FCS.CLA.199	H4	0.4	0.45	126	Sternal segment portion, Rib 6	1	1	Complete	Left
FCS.CLA.200	H4	0.73	0.28	121.5	Sternal segment portion, Rib 3	1	1	Complete	Left
FCS.CLA.201	H4	0.05	0.69	120.5	Pelvis	1	1	Fragment	-
FCS.CLA.202	H4	0.21	0.53	125.5	Patella	1	1	Complete	Left
FCS.CLA.205	H4	0.55	0.45	123	Hyoid apparatus	1	1	Complete	Axial
FCS.CLA.206	H4	0.41	0.41	130	Sternum	1	1	Complete	Axial
FCS.CLA.208	H5	0.39	0.63	117	Metacarpal II	1	1	Fragment	Left
FCS.CLA.209	H5	0.39	0.23	115.5	Metacarpal III	1	1	Complete	Right
FCS.CLA.210	H5	0.24	0.28	113.5	Mesocuneiform (hindlimb)	1	1	Fragment	Right
FCS.CLA.211	H5	0.2	0.79	116.5	Metacarpal III	1	1	Complete	Right
FCS.CLA.214	H6	0.92	0.78	121.5	Phalanx 1-2-III (forelimb)	1	1	Fragment	-
FCS.CLA.220	I3	0.46	0.45	114.5	Carpal	1	1	Fragment	-
FCS.CLA.221	I3	0.33	0.79	117	Pisiform (forelimb)	1	1	Complete	Right
FCS.CLA.222	I4	0.25	0.32	110.5	Sternal segment portion, Rib 4	1	1	Fragment	Right
FCS.CLA.223	I4	0.89	0.18	128	Phalanx 1-2-III (hindlimb)	1	1	Fragment	Left
FCS.CLA.224	I4	0.96	0.25	125	Phalanx 1-2-III (hindlimb)	1	1	Fragment	Right
FCS.CLA.225	I5	0.99	0.04	113	Phalanx 1-IV (forelimb)	1	1	Complete	Left
FCS.CLA.226	I5	0.15	0.94	113	Rib	1	-	Fragment	-
FCS.CLA.962	H0	-	-	-	Tooth	1	1	Fragment	-
FCS.CLA.1912	No data	-	-	-	Tooth	1	-	Fragment	-
FCS.CLA.1947	Surface	-	-	-	Rib	1	-	Fragment	-
FCS.CLA.1948	Surface	-	-	-	Rib	1	-	Fragment	-

FCS.CLA.1950	Surface	-	-	-	Rib	1	1	Fragment	-
FCS.CLA.1972	F2	-	-	-	Caudal vertebra	1	1	Fragment	Axial
FCS.CLA.1975	No data	-	-	-	Femur	1	1	Complete	Right
FCS.CLA.1976	No data	-	-	-	Caudal vertebra 1	1	1	Fragment	Axial
FCS.CLA.1977	No data	-	-	-	Rib	1	-	Fragment	-
FCS.CLA.1979	I-5	0	0.85	125	Phalanx 1-II	1	1	Complete	Left
FCS.CLA.1991	H7	0.17	0.65	99	Rib	1	-	Fragment	-
FCS.CLA.1992	J2	0.74	0.59	110	Autopodial	1	1	Complete	
FCS.CLA.1993	I7	0.77	0.68	105	Distal carpal external 4+5 (forelimb)	1	1	Complete	Right
Total	**-**	**-**	**-**	**-**	**-**	**111**	**81**	**-**	**-**
Neosclerocalyptus **sp.**									
FCS.CLA.69	G4	0.46	0	106	Humerus	1	1	Fragment	Left
Doedicurus **sp.**									
FCS.CLA.6	G2	0.70	0.13	122,5	Femur	1	1	Fragment	Left

Table S2. Stratigraphic and anatomical data for skeletal elements (MNE) of modern fauna recovered from Campo Laborde.

Catalogue number	Grid	Level BGL	Element	Condition	Laterality
Dolichotis patagonum					
FCS.CLA.227	G5	90-95	Tibia	Fragment	Left
FCS.CLA.228	H4	105-110	Calcaneus	Complete	Right
FCS.CLA.1735	F6	125-130	Phalanx I	Complete	Right
FCS.CLA.1759	G1	125-130	Tarsian I	Complete	Right
FCS.CLA.1516	I1	130-135	Phalanx II	Complete	Right
FCS.CLA.700	F4	130-135	Phalanx III	Complete	Right
FCS.CLA.903	G5	130-135	Tarsian 3	Complete	Left
FCS.CLA.1518	I1	135-140	Tarsian I	Fragment	Left
FCS.CLA.491	E4	100-105	Molar	Complete	-
FCS.CLA.830	G4	115-120	Molar	Fragment	-
FCS.CLA.461A	E3	125-130	Molar	Fragment	-
FCS.CLA.461B	E3	125-130	Molar	Fragment	-
FCS.CLA.698	F4	130-135	Molar 3	Fragment	Left
FCS.CLA.699	F4	130-135	Molar 1	Fragment	Left
Lagostomus maximus					
FCS.CLA.117	H5	90-95	Mandible	Fragment	Left
FCS.CLA.138	I3	95-100	Maxilla	Complete	Axial
FCS.CLA.158	E3	125-130	Femur	Fragment	Left
FCS.CLA.774	F6	125-130	Rib	Fragment	Right
FCS.CLA.1610	I3	135-140	Astragalus	Fragment	Right
FCS.CLA.1856	F3	140-145	Astragalus	Complete	Right
FCS.CLA.1875	-	-	Phalanx	Complete	-
FCS.CLA.2007	L1	90-95	Mandible	Fragment	-
Dasypodidae					
FCS.CLA.1477	I1	80-90	Phalanx	Complete	-
FCS.CLA.1478	I1	80-90	Fixed plate	Fragment	Caparazón
FCS.CLA.1286	H5	90-95	Phalanx	Fragment	-
FCS.CLA.1714	I6	95-100	Phalanx	Complete	-
FCS.CLA.871	G5	100-105	Plate	Fragment	Axial
FCS.CLA.553	E5	110-115	Mobil plate	Fragment	Axial
FCS.CLA.1639	I4	110-115	Phalanx	Complete	-
FCS.CLA.1164	H3	110-115	Phalanx	Complete	-
FCS.CLA.835	G4	115-120	Phalanx	Complete	-
FCS.CLA.735	F5	115-120	Phalanx	Complete	-
FCS.CLA.1700	I5	125-130	Phalanx	Complete	-
FCS.CLA.1566	I2	130-135	Phalanx	Complete	-
FCS.CLA.1657	I4	130-135	Fixed plate	Complete	Axial
FCS.CLA.1601	I3	130-135	Phalanx	Complete	-
FCS.CLA.1120	H2	130-135	Phalanx	Complete	-
FCS.CLA.1466	I0	130-135	Humerus	Fragment	Right
FCS.CLA.1281	H4	130-135	Phalanx	Complete	-
FCS.CLA.1424	I0	135-140	Phalanx	Complete	-
FCS.CLA.832C	G4	115-120	Molar	Fragment	-

FCS.CLA.1876	-	-	Articular	Complete	-
Zaedyus pichiy					
FCS.CLA.1490	I1	95-100	Mobil plate	Fragment	Axial
FCS.CLA.1097	H2	120-125	Mobil plate	Fragment	Axial
FCS.CLA.783	G1	135-140	Mobil plate	Fragment	Axial
FCS.CLA.1433	I0	85-90	Mobil plate	Complete	Axial
Lycalopex sp.					
FCS.CLA.1040	H1	105-110	Premolar 1	Complete	Right
FCS.CLA.1583	I3	100-105	Canine	Complete	-
Canidae					
FCS.CLA.1448	I0	110-115	Phalanx	Complete	-
FCS.CLA.1304	H5	110-115	Phalanx	Complete	-
FCS.CLA.1305	H5	110-115	Phalanx	Complete	-
FCS.CLA.1306	H5	110-115	Metapodial	Fragment	-
FCS.CLA.965	H0	120-125	Phalanx	Complete	-
FCS.CLA.773	F6	125-130	Phalanx	Complete	-
FCS.CLA.572	E5	125-130	Phalanx	Complete	-
FCS.CLA.1267	H4	125-130	Phalanx	Complete	-
FCS.CLA.1815	G3	130-135	Phalanx	Complete	-
FCS.CLA.1799	G2	140-145	Phalanx	Complete	-
Tayassu sp.					
FCS.CLA.82	G5	105-110	Radio-ulna	Complete	Left
Lama guanicoe					
FCS.CLA.2006	K4	110-115	Cervical vertebra	Fragment	Axial
Camelidae					
FCS.CLA.36	F3	130-135	Patella	Fragment	Right
FCS.CLA.43	E6	90-95	Autopodial	Fragment	-
FCS.CLA.87	H1	100-105	Rib	Fragment	Right

Table S3. Previous AMS ^{14}C dates from Campo Laborde.

Catalogue Number	Year Reported	Lab Number	Material Dated	Description	Taxon	Chemical Fraction Dated	^{14}C Age ± 1 SD RC years BP	Ref.
FCS.CLA.1979	2007	AA-71667	Bone	Phalanx 1-II	*Megatherium americanum*	ABA Treated Bone	6,740 ± 480	(20)
FCS.CLA.9	2012	CAMS-155863	Bone	Rib	*Megatherium americanum*	UF-Gelatin	7,380 ± 410	(47)
FCS.CLA.211	2007	AA-71666	Bone	Metacarpal III	*Megatherium americanum*	ABA Treated Bone	7,630 ± 460	(20)
FCS.CLA.28	2006	AA-55117	Bone	Rib	*Megatherium americanum*	Gelatinized HCl-insoluble residue	7,750 ± 250	(20)
FCS.CLA.99	2006	AA-55118	Bone	Rib	*Megatherium americanum*	Gelatinized HCl-insoluble residue	8,080 ± 200	(20)
FCS.CLA.100	2006	AA-55119	Bone	Long bone	Megamammal	Gelatinized HCl-insoluble residue	8,720 ± 190	(20)
FCS.CLA.154	2007	AA-71665	Bone	Metacarpal V	*Megatherium americanum*	ABA Treated Bone	9,730 ± 290	(20)

Table S4. AMS radiocarbon measurements for known-age samples and backgrounds.

AMS Lab No.	Chemical Fraction Dated	^{14}C years BP ± 1 SD	Consensus Value ^{14}C years BP	Reference
TIRI- Whalebone				
CAMS-171442	XAD-2 purified hydrolyzate of gelatin from KOH-extracted collagen	12,695 ± 40	12,788 ± 30	(*48*)
CAMS-172433	XAD-2 purified hydrolyzate of gelatin from KOH-extracted collagen	12,795 ± 35	12,788 ± 30	(*48*)
EL 10-145 Bone				
CAMS-171445	XAD-2 purified hydrolyzate of gelatin from KOH-extracted collagen	53,180 ±300	> 50,000	(*A*)
CAMS-172434	XAD-2 purified hydrolyzate of gelatin from KOH-extracted collagen	49,450 ± 200	> 50,000	(*A*)
ACT III Bone				
CAMS-171443	XAD-2 purified hydrolyzate of gelatin from KOH-extracted collagen	8305 ± 35	~8,350	(*B*)
CAMS-172435	XAD-2 purified hydrolyzate of gelatin from KOH-extracted collagen	8300 ± 35	~8,350	(*B*)

(*48*) Table 6.1b (page 328). (*A*) Internal LLNL Laboratory standard – Bison priscus bone, Klondike – Yukon Territory (Canada). Tom Guilderson, personal communication 24 April 2018. (*B*) Internal LLNL Laboratory standard – whale vertebra, Svenskoya – Svalbard (Norway). Tom Guilderson, personal communication 25 April 2018.